

## *Supporting Information for*

# **Bibliometric analysis of photocatalytic oxidation for volatile organic compounds from 1998 to 2023**

Xinjie Zhu <sup>a</sup>, Yifan Sui <sup>a</sup>, Xiuli Li <sup>a</sup>, Jie Guan <sup>a</sup>, Xiaojiao Zhang <sup>a,\*</sup>, Gangfeng Zhang <sup>b</sup>, and Yaoguang Guo <sup>a,\*</sup>

<sup>a</sup> *Shanghai Collaborative Innovation Centre for WEEE Recycling, School of Resources and Environmental Engineering, Shanghai Polytechnic University, Shanghai 201209, China; zhuxinjie1231@163.com (X. Zhu); suiyifan333@163.com; [xli@sspu.edu.cn](mailto:xli@sspu.edu.cn) (X. Li); guanjie@sspu.edu.cn (J. Guan); xjzhang@sspu.edu.cn (X. Zhang); ygguo@sspu.edu.cn (Y. Guo)*

<sup>b</sup> *Shanghai Academy of Environmental Sciences, Shanghai 200233, China; gf.zh@foxmai.com (G. Zhang)*

\* Corresponding authors.

E-mail addresses: [xjzhang@sspu.edu.cn](mailto:xjzhang@sspu.edu.cn) (X. Zhang); [ygguo@sspu.edu.cn](mailto:ygguo@sspu.edu.cn) (Y. Guo)

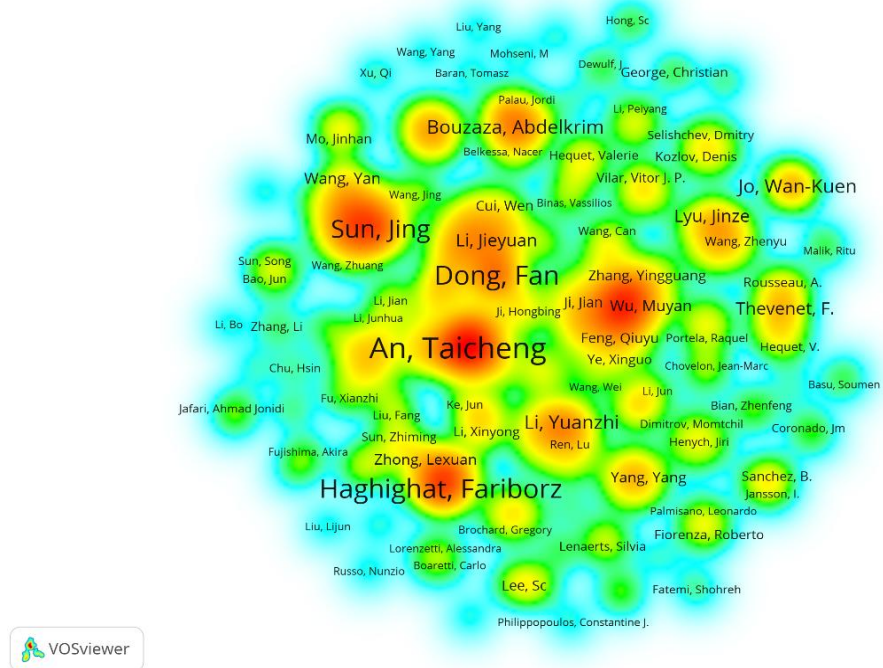


**Figure S1.** Strength of linkage map between authors in the field of photocatalytic oxidation of VOCs.

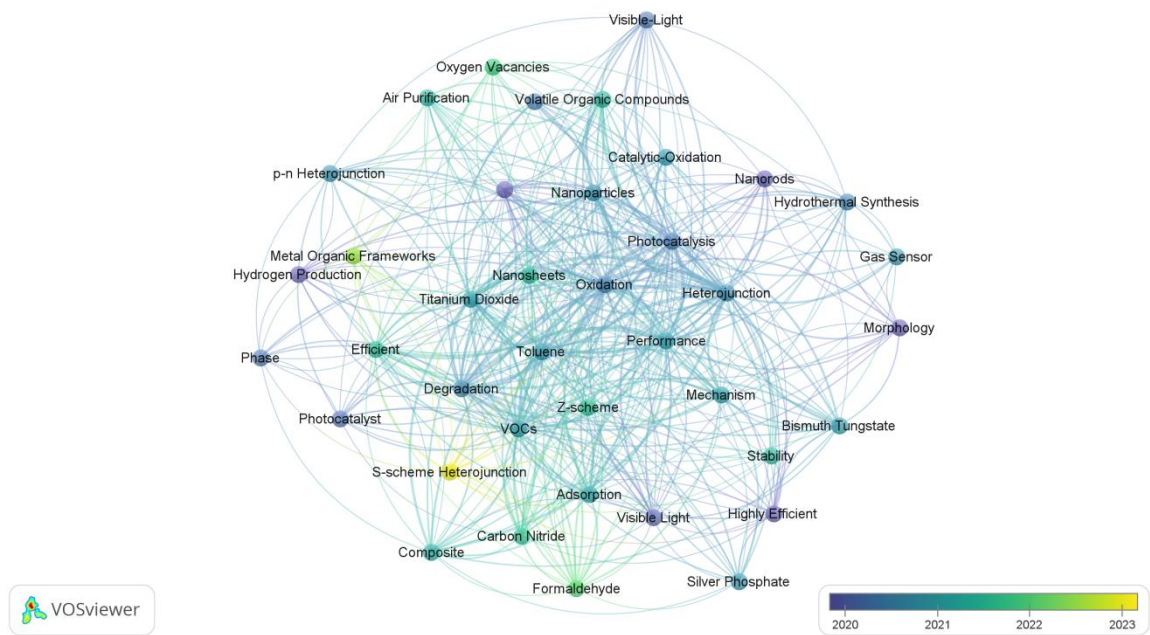


**Figure S2.** Keywords analysis of heterojunction strategies in photocatalytic degradation of VOCs.

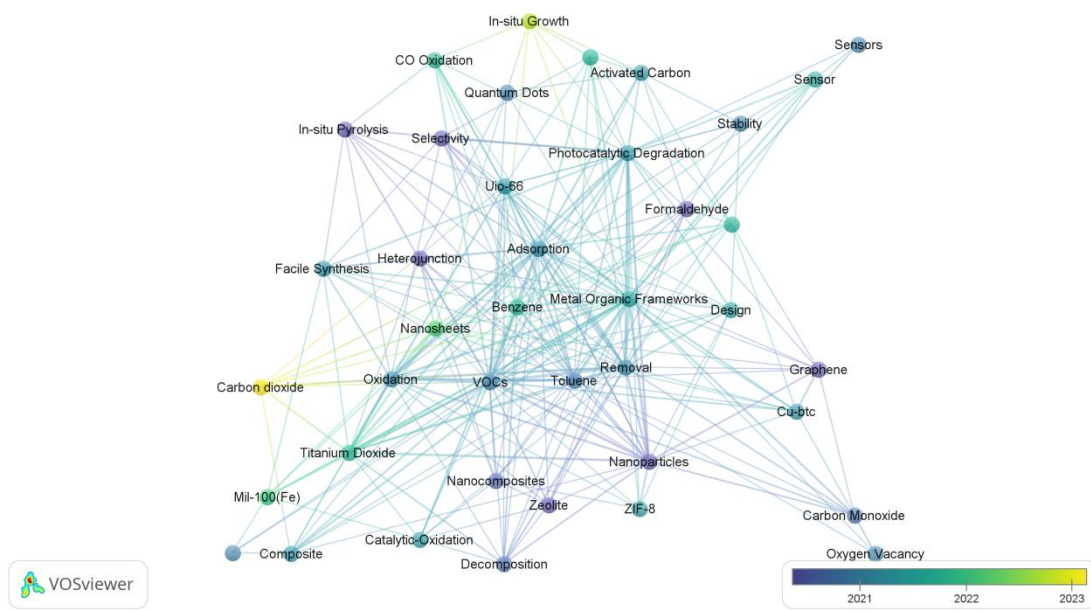


**Figure S3.** Keywords analysis of MOFs in photocatalytic degradation of VOCs.

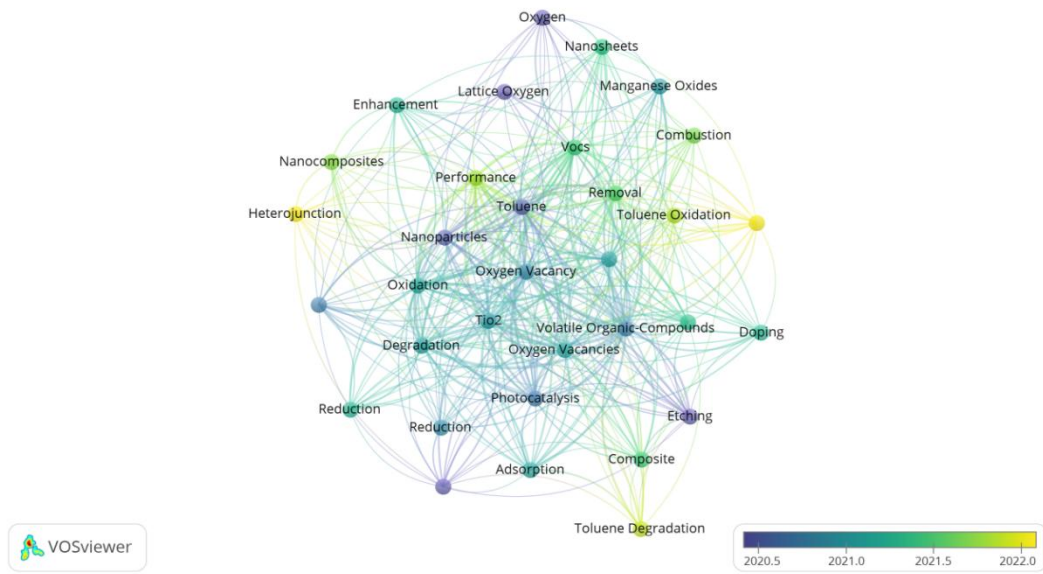


**Figure S4.** Keywords analysis of Oxygen vacancy in photocatalytic degradation of VOCs.

**Table S1.** Number of publications, citations and total linkage strength of each country.

Country	Documents	Citations	Total link strength
China	1144	46702	325
USA	226	18463	185
France	205	7567	125
South Korea	198	6417	121
India	124	3361	118
Japan	122	5802	70
Canada	101	4537	54
Spain	98	4123	69
Iran	86	4552	40
Italy	77	5329	57

**Table S2.** Top 10 most cited articles

No.	Title	Author	Year	Citations	References
1	Photoinduced reactivity of titanium dioxide	Carp, O., et al.	2004	4160	[1]
2	A review on the visible light active titanium dioxide photocatalysts for environmental applications	Pelaez, M., et al.	2012	3342	[2]
3	Fundamentals and Catalytic Applications of CeO <sub>2</sub> -Based Materials	Montini, T., et al.	2016	1800	[3]
4	Defective TiO <sub>2</sub> with oxygen vacancies: synthesis, properties and photocatalytic applications	Pan, X., et al.	2013	1614	[4]
5	Protocol for the development of the Master Chemical Mechanism, MCM v3 (Part A): tropospheric degradation of non-aromatic volatile organic compounds	Saunders, S.M., et al.	2003	936	[5]

6	Photocatalytic oxidation for indoor air purification: a literature review	Zhao, J., et al.	2003	883	[6]
7	Photocatalytic purification of volatile organic compounds in indoor air: A literature review	Mo, J., et al.	2009	756	[7]
8	TiO <sub>2</sub> photocatalyst for removal of volatile organic compounds in gas phase-A review	Shayegan, Z., et al.	2017	712	[8]
9	Titanium Dioxide Photocatalysis in Atmospheric Chemistry	Chen, H., et al.	2012	668	[9]
10	Low temperature catalytic oxidation of volatile organic compounds: a review	Huang, H., et al.	2015	564	[10]

**Table S3.** Treatment processes for the removal of VOCs.

Photocatalyst	Synthetic precursor	Target pollutants	Eg(eV)	Ref.
TiO <sub>2</sub>	/	benzyl alcohol	3.2	[11]
F-TiO <sub>2</sub>	C <sub>16</sub> H <sub>36</sub> O <sub>4</sub> Ti, HF	toluene	/	[12]
Pd/TiO <sub>2</sub>	Pd(OAc) <sub>2</sub> , TiO <sub>2</sub>	benzene	/	[13]
F-0.5%Ce-TiO <sub>2</sub>	TiOSO <sub>4</sub> · xH <sub>2</sub> O+H <sub>2</sub> SO <sub>4</sub> , Ce(NO <sub>3</sub> ) <sub>3</sub> · 6H <sub>2</sub> O, NH <sub>4</sub> F	methyl ethyl ketone	3.0	[14]
TiO <sub>2</sub> /H <sub>2</sub> Ti <sub>3</sub> O <sub>7</sub>	SiO <sub>2</sub> , C <sub>12</sub> H <sub>28</sub> O <sub>4</sub> Ti	toluene and acetone	3.3	[15]
TiO <sub>2</sub> /Pd	Commercial TiO <sub>2</sub> powder, Pd(NO <sub>3</sub> ) <sub>2</sub>	<i>n</i> -octane, isooctane, <i>n</i> -hexane, and cyclohexane	2.8	[16]
Cu <sub>2</sub> O/CuO/TiO <sub>2</sub>	Ti(OBu) <sub>4</sub> , Cu (NO <sub>3</sub> ) <sub>2</sub> · 3H <sub>2</sub> O	acetone	/	[17]
bentonite/M-TiO <sub>2</sub> (M= Au, Ag and Pd)	AgNO <sub>3</sub> , HAuCl <sub>4</sub> , PdCl <sub>2</sub> , NaBH <sub>4</sub>	benzaldehyde	2.93, 2.95, 2.98	[18]
Au/TiO <sub>2</sub> -CeO <sub>2</sub>	Ce(NO <sub>3</sub> ) <sub>3</sub> · 6H <sub>2</sub> O, HAuCl <sub>4</sub>	2-propanol	/	[19]
C-TiO <sub>2</sub>	carbon black, P25-TiO <sub>2</sub>	methyl ethyl ketone	2.35	[20]
N@S-TiO <sub>2</sub>	C <sub>12</sub> H <sub>28</sub> O <sub>4</sub> Ti, CH <sub>4</sub> N <sub>2</sub> S	ethano	2.93	[21]
F-FeTi-0.4%	TiOSO <sub>4</sub> · xH <sub>2</sub> O+H <sub>2</sub> SO <sub>4</sub> , FeSO <sub>4</sub> · 7H <sub>2</sub> O	methyl ethyl ketone	2.89	[22]
Pd/TiO <sub>2</sub>	PdCl <sub>2</sub> , P25-TiO <sub>2</sub>	formaldehyde,	/	[23]

			toluene and xylenes		
Mn/meso-TiO <sub>2</sub>	C <sub>16</sub> H <sub>36</sub> O <sub>4</sub> Ti, (CH <sub>3</sub> COO) <sub>2</sub> Mn	benzene	/	[24]	
TiO <sub>2</sub> -WO <sub>3</sub>	C <sub>16</sub> H <sub>36</sub> O <sub>4</sub> Ti, H <sub>2</sub> WO <sub>4</sub>	xylene	/	[25]	
Mn <sup>2+</sup> /USTiO <sub>2</sub>	C <sub>16</sub> H <sub>36</sub> O <sub>4</sub> Ti, MnCl <sub>2</sub> ·4H <sub>2</sub> O	toluene	/	[26]	
Ag <sub>2</sub> CO <sub>3</sub> -TiO <sub>2</sub> -GO	GO, Ag <sub>2</sub> CO <sub>3</sub> , TiO <sub>2</sub>	o-xylene	2.62	[27]	
Er <sub>1</sub> -TiO <sub>2</sub> /La <sub>1</sub> -TiO <sub>2</sub>	La(NO <sub>3</sub> ) <sub>3</sub> ·nH <sub>2</sub> O, Er(NO <sub>3</sub> ) <sub>3</sub> ·6H <sub>2</sub> O, C <sub>12</sub> H <sub>28</sub> O <sub>4</sub> Ti	methanol and acetaldehyde	/	[28]	
CQDs/TiO <sub>2</sub>	C <sub>16</sub> H <sub>36</sub> O <sub>4</sub> Ti, HF, C <sub>6</sub> H <sub>8</sub> O <sub>7</sub>	benzene, p-xylene, and toluene	3.12	[29]	
BiVO <sub>4</sub> /TiO <sub>2</sub>	Bi(NO <sub>3</sub> ) <sub>3</sub> ·5H <sub>2</sub> O, Ti(OiPr) <sub>4</sub>	benzene	2.87	[30]	
TiO <sub>2</sub> /SiO <sub>2</sub> /Bi <sub>2</sub> O <sub>3</sub>	SiO <sub>2</sub> , Bi(NO <sub>3</sub> ) <sub>3</sub> ·5H <sub>2</sub> O, TiOSO <sub>4</sub>	benzene	2.8	[31]	
Fe-TiO <sub>2</sub>	Ti(OC <sub>4</sub> H <sub>9</sub> ) <sub>4</sub> , Fe(NO <sub>3</sub> ) <sub>3</sub>	toluene	2.96	[32]	
N-TiO <sub>2</sub>	N(CH <sub>2</sub> CH <sub>3</sub> ) <sub>3</sub> , HNO <sub>3</sub> , Ti(OC <sub>4</sub> H <sub>9</sub> ) <sub>4</sub>	toluene	3.0	[33]	
TiBi <sub>x</sub> Zn <sub>y</sub> O <sub>2</sub>	Bi(NO <sub>3</sub> ) <sub>3</sub> ·5H <sub>2</sub> O, Zn(NO <sub>3</sub> ) <sub>2</sub> ·6H <sub>2</sub> O;TiOSO <sub>4</sub>	toluene	2.54	[34]	
Cu <sub>2</sub> O/TiO <sub>2</sub>	NiCl <sub>2</sub> ·6H <sub>2</sub> O, Ti(OBu) <sub>4</sub>	toluene	2.08/2.77	[35]	
Ni-TiO <sub>2</sub> /SnO <sub>2</sub>	Ti(OBu) <sub>4</sub> , NiCl <sub>2</sub> ·6H <sub>2</sub> O, (C <sub>6</sub> H <sub>5</sub> ) <sub>3</sub> Sn-OH	toluene	/	[36]	
N-TiO <sub>2</sub>	TiCl <sub>3</sub> , CO(NH <sub>2</sub> ) <sub>2</sub>	formaldehyde	/	[37]	
Pt/TiO <sub>2</sub>	H <sub>2</sub> PtCl <sub>6</sub> ·6H <sub>2</sub> O, C <sub>16</sub> H <sub>36</sub> O <sub>4</sub> Ti	NO <sub>x</sub>	2.73	[38]	
TiO <sub>2</sub> /HAp	TiCl <sub>4</sub> , (NH <sub>4</sub> ) <sub>2</sub> HPO <sub>4</sub> , NH <sub>3</sub> ·H <sub>2</sub> O, Ca(NO <sub>3</sub> ) <sub>2</sub> ·4H <sub>2</sub> O, C <sub>2</sub> H <sub>6</sub> O	NO	/	[39]	
UO <sub>2</sub> <sup>2+</sup> /TiO <sub>2</sub>	UO <sub>2</sub> (NO <sub>3</sub> ) <sub>2</sub> , TiO <sub>2</sub> powder	acetone, cyclohexane alcohols, ethanol and propan-2-ol	/	[40]	
g-C <sub>3</sub> N <sub>4</sub> /Ag-TiO <sub>2</sub>	C <sub>3</sub> H <sub>6</sub> N <sub>6</sub> , AgNO <sub>3</sub> , P25 TiO <sub>2</sub>	acetaldehyde	2.70	[41]	
NCDs@TiO <sub>2</sub>	C <sub>6</sub> H <sub>8</sub> O <sub>7</sub> , CO(NH <sub>2</sub> ) <sub>2</sub> , AgNO <sub>3</sub> , HF, C <sub>16</sub> H <sub>36</sub> O <sub>4</sub> Ti, NaBH <sub>4</sub>	toluene	3.27	[42]	
GF-Fe-TiO <sub>2</sub>	Ti[O(CH <sub>2</sub> ) <sub>3</sub> CH <sub>3</sub> ] <sub>4</sub> , Fe(NO) <sub>3</sub> , glass fibers	benzene, toluene, ethylbenzene, and o-xylene	/	[43]	



N-TiO <sub>2</sub>	Ti (OCH <sub>2</sub> CH <sub>2</sub> CH <sub>3</sub> ) <sub>4</sub> , NF	ethylbenzene	2.91	[44]
N-TiO <sub>2</sub>	C <sub>2</sub> H <sub>4</sub> N <sub>4</sub> , P25-TiO <sub>2</sub>	benzene	2.57-2.91	[45]
F-TiO <sub>2</sub>	NH <sub>4</sub> HF <sub>2</sub> , C <sub>16</sub> H <sub>36</sub> O <sub>4</sub> Ti	toluene	/	[46]
MnO <sub>2</sub> /TiO <sub>2</sub>	C <sub>16</sub> H <sub>36</sub> O <sub>4</sub> Ti, KMnO <sub>4</sub>	toluene	2.25	[47]
Fe <sub>2</sub> O <sub>3</sub> /TiO <sub>2</sub>	Fe(NO <sub>3</sub> ) <sub>3</sub> ·9H <sub>2</sub> O, P25-TiO <sub>2</sub>	acetaldehyde and o-xylene	2.3	[48]
CuO/TiO <sub>2</sub>	Cu(NO <sub>3</sub> ) <sub>2</sub> ·3H <sub>2</sub> O, H <sub>3</sub> BTC (BTC = 1, 3, 5-benzoic acid), DMSO, Anatase TiO <sub>2</sub>	xylene	2.68-2.75	[49]
ZnO/TiO <sub>2</sub>	Zn(CH <sub>3</sub> COO) <sub>2</sub> ·2H <sub>2</sub> O, P25-TiO <sub>2</sub>	toluene	2.95	[50]
TiO <sub>2</sub> -CeO <sub>2</sub>	Ce(OH) <sub>4</sub> , CHO <sub>4</sub> Ti	toluene	2.54	[51]
Pt-MoS <sub>2</sub> /TiO <sub>2</sub>	TiCl <sub>4</sub> , (NH <sub>4</sub> ) <sub>6</sub> Mo <sub>7</sub> O <sub>24</sub> ·4H <sub>2</sub> O, CH <sub>4</sub> N <sub>2</sub> S, K <sub>2</sub> PtCl <sub>6</sub>	toluene	/	[52]
CuS/TiO <sub>2</sub>	Na <sub>2</sub> S, Cu(NO <sub>3</sub> ) <sub>2</sub>	toluene	2.77	[53]
CdS/TiO <sub>2</sub>	Cd(NO <sub>3</sub> ) <sub>2</sub> , Na <sub>2</sub> S	benzene	3.01	[53]
CuS-CdS/TiO <sub>2</sub>	Cd(NO <sub>3</sub> ) <sub>2</sub> , Na <sub>2</sub> S, Cd(NO <sub>3</sub> ) <sub>2</sub>	toluene	2.55	[53]
CdS/TiO <sub>2</sub>	CdCl <sub>2</sub> , Na <sub>2</sub> S·9H <sub>2</sub> O	benzene	2.2	[54]
CdSe/TiO <sub>2</sub>	CdCl <sub>2</sub> , selenium powder	acetaldehyde	2.4	[54]
CdTe/TiO <sub>2</sub>	Na <sub>2</sub> TeO <sub>3</sub> , CdCl <sub>2</sub>	acetaldehyde	2.8	[54]
(Mn)g-C <sub>3</sub> N <sub>4</sub> /TiO <sub>2</sub>	C <sub>16</sub> H <sub>36</sub> O <sub>4</sub> Ti, C <sub>3</sub> H <sub>6</sub> N <sub>6</sub> , Mn(NO <sub>3</sub> ) <sub>2</sub> ·4H <sub>2</sub> O	benzene	3.12	[55]
LaVO <sub>4</sub> /TiO <sub>2</sub>	La(NO <sub>3</sub> ) <sub>3</sub> , NH <sub>4</sub> VO <sub>3</sub> , TiO <sub>2</sub>	toluene	2.1	[56]
Ag-ZnO	AgNO <sub>3</sub> , Zn(NO <sub>3</sub> ) <sub>2</sub> ·6H <sub>2</sub> O	benzene, toluene, and xylene	/	[57]
ZnO-rGO	Zn(OAc) <sub>2</sub> , GO	phenol and acetone	/	[58]
Fe/ZnO	FeCl <sub>3</sub> ·6H <sub>2</sub> O, ZnCl <sub>2</sub>	toluene and nitrobenzene	/	[59]
ZnO-X/ND	ZnO, Pure nanodiamond	formaldehyde	3.25	[60]
Ag/F-SrTiO <sub>3</sub>	Ti(C <sub>4</sub> H <sub>9</sub> O) <sub>4</sub> , Sr(NO <sub>3</sub> ) <sub>2</sub> , NH <sub>4</sub> F	aromatics	2.86	[61]
ZnIn <sub>2</sub> S <sub>4</sub> /In <sub>2</sub> O <sub>3</sub>	InCl <sub>3</sub> , ZnIn <sub>2</sub> S <sub>4</sub>	toluene	2.17	[62]

Ni-g-C <sub>3</sub> N <sub>4</sub>	C <sub>3</sub> H <sub>6</sub> N <sub>6</sub> , Ni(NO <sub>3</sub> ) <sub>2</sub>	toluene	2.25	[63]
Biochar/MnO <sub>2</sub> /g-C <sub>3</sub> N <sub>4</sub>	(C <sub>6</sub> HO <sub>5</sub> ) <sub>n</sub> , KMnO <sub>4</sub>	toluene	2.23	[64]
H <sub>3</sub> PW <sub>12</sub> O <sub>40</sub> /g-C <sub>3</sub> N <sub>4</sub>	CH <sub>4</sub> N <sub>2</sub> O, C <sub>8</sub> H <sub>12</sub> O <sub>8</sub> Si, H <sub>3</sub> PW <sub>12</sub> O <sub>40</sub>	toluene	2.78	[65]
α-MnO <sub>2</sub> /Mn <sub>3</sub> O <sub>4</sub>	MnCO <sub>3</sub> , MnSO <sub>4</sub>	phenol and toluene	1.82	[66]
CeO <sub>2</sub>	Ce(NO <sub>3</sub> ) <sub>3</sub> ·H <sub>2</sub> O, CH <sub>4</sub> N <sub>2</sub> O	toluene	2.86-2.97	[67]
CaTiO <sub>3</sub>	CaZnTiO <sub>3</sub>	toluene	3.2	[68]
Eu <sup>3+</sup> -CaTiO <sub>3</sub>	CaZnTiO <sub>3</sub> , Eu(NO <sub>3</sub> ) <sub>3</sub> ·6H <sub>2</sub> O	toluene	3.0	[68]
Pt/SrTiO <sub>3</sub>	Ti(C <sub>4</sub> H <sub>9</sub> O) <sub>4</sub> , Sr(NO <sub>3</sub> ) <sub>2</sub> , H <sub>2</sub> PtCl <sub>6</sub>	toluene	1.92	[69]
BaZrO <sub>3</sub>	ZrOCl <sub>2</sub> ·8H <sub>2</sub> O, C <sub>19</sub> H <sub>42</sub> BrN	toluene	4.8	[70]
SrZrO <sub>3</sub>	C <sub>19</sub> H <sub>42</sub> BrN, Sr(NO <sub>3</sub> ) <sub>2</sub>	benzyl alcohol	/	[70]
Pt/Er-KTaO <sub>3</sub>	Ta <sub>2</sub> O <sub>5</sub> , KOH, H <sub>2</sub> PtCl <sub>6</sub> , Er(NO <sub>3</sub> ) <sub>3</sub> ·5H <sub>2</sub> O	toluene	3.34	[71]
ZnFe <sub>2</sub> O <sub>4</sub>	Zn(NO <sub>3</sub> ) <sub>2</sub> ·6H <sub>2</sub> O, Fe(NO <sub>3</sub> ) <sub>3</sub> ·6H <sub>2</sub> O	benzene	1.87	[72]
Pt/Bi <sub>2</sub> WO <sub>6</sub>	Bi(NO <sub>3</sub> ) <sub>3</sub> ·5H <sub>2</sub> O, Na <sub>2</sub> WO <sub>4</sub> ·2H <sub>2</sub> O, H <sub>2</sub> PtCl <sub>6</sub> ·6H <sub>2</sub> O	methyl ethyl ketone	2.33	[73]
BiVO <sub>4</sub>	Bi(NO <sub>3</sub> ) <sub>3</sub> ·5H <sub>2</sub> O, NH <sub>4</sub> VO <sub>3</sub>	toluene and acetone	2.17	[74]
CuS-CdS-(BiO) <sub>2</sub> CO <sub>3</sub>	Bi(NO <sub>3</sub> ) <sub>3</sub> ·5H <sub>2</sub> O; Cu(NO <sub>3</sub> ) <sub>2</sub> ·6H <sub>2</sub> O; Cd(NO <sub>3</sub> ) <sub>2</sub> ·6H <sub>2</sub> O	<i>n</i> -octane, isooctane, <i>n</i> -hexane, and cyclohexane	2.25	[75]

**Table S4.** Heterojunction strategy in photocatalytic degradation of VOCs.

Scheme	Photocatalyst	Eg(eV)	Target pollutants	Pollutant Degradation Effect	Ref.
p-n	Co <sub>3</sub> O <sub>4</sub> /TiO <sub>2</sub>	2.02	Toluene	90% (100mg catalyst; 300W Xe Lamp; 200°C)	[76]
p-n	CoO/WO <sub>3</sub>	2.43	toluene	85.4% (20mg catalyst; 300W Xe Lamp; 4h)	[77]
p-n	graphene oxide-TiO <sub>2</sub>	2.9-3.15	Methanol	90% (10mg catalyst; UV Light; 5h)	[78]
p-n	α-Fe <sub>2</sub> O <sub>3</sub> /CaFeO	/	Acetaldehyde	80% (50mg catalyst; Xe Lamp; 180min)	[79]
p-n	Ag/Ag <sub>2</sub> O@Ti	/	toluene	99.1% (0.01 g/cm <sup>2</sup> catalyst;	[80]

	O <sub>2</sub>				256nm UV Light; 1h)	
p-n	LaVO <sub>4</sub> /BiOBr	2.63	toluene and acetone		95.4% and 87.1% (0.2g catalyst; 500W Xe Lamp;	[81]
p-n	CuInS <sub>2</sub> /Bi <sub>2</sub> WO <sub>6</sub>	2.6	toluene		90% (0.2g catalyst; 500 W Xe lamp;5h)	[82]
p-n	Co <sub>3</sub> O <sub>4</sub> /TiO <sub>2</sub>	/	benzene		95% (0.1g catalyst; UV Light; 40min)	[83]
p-n	TiO <sub>2</sub> -Cu <sub>2</sub> O	2.08	toluene		90% (50mg catalyst; 500W Xe Lamp; 180min)	[84]
Z-scheme	Ag <sub>3</sub> PO <sub>4</sub> -g-C <sub>3</sub> N <sub>4</sub>	2.7	toluene		87.52% (300mg catalyst; Xe Lamp; 100min)	[85]
Z-scheme	Ag/Ag <sub>3</sub> PO <sub>4</sub> /C	/	C <sub>6</sub> H <sub>6</sub>		90.18% (300W Xe Lamp; 3h)	[86]
Z-scheme	Ag/WO <sub>3</sub> /Bi <sub>2</sub> WO <sub>6</sub>	2.57	chlorobenzene		80% (0.2g catalyst; 300W Xe Lamp; 10h)	[87]
Z-scheme	MnO <sub>2</sub> /g-C <sub>3</sub> N <sub>4</sub>	2.54	formaldehyde		91.78% (0.3g catalyst; 500W Xe Lamp; 3h)	[88]
Z-scheme	Bi <sub>2</sub> WO <sub>6</sub> /BiOC	2.49	toluene		99% (0.2g catalyst; 350 W Xe Lamp; 3h)	[89]
Z-scheme	WO <sub>3</sub> /Bi <sub>2</sub> WO <sub>6</sub>	/	toluene		92% (0.2g catalyst; 300 W Xe Lamp; 1h)	[90]
Z-scheme	g-C <sub>3</sub> N <sub>4</sub> /Bi <sub>2</sub> WO <sub>6</sub>	2.53	toluene		93.6% (0.4g/cm <sup>2</sup> catalyst; 300 W Xe Lamp;2h)	[91]
Z-scheme	MnO <sub>2</sub> /g-C <sub>3</sub> N <sub>4</sub>	/	formaldehyde		100% (50mg catalyst; 300 W Xe Lamp; 1.5h)	[92]
S-scheme	tubular g-C <sub>3</sub> N <sub>4</sub> /BiVO <sub>4</sub>	/	formaldehyde		95.4%(3g catalyst; 500 W Xe Lamp; 40min)	[93]
S-scheme	CdS/Bi <sub>2</sub> MoO <sub>6</sub>	/	C <sub>2</sub> H <sub>4</sub>		100% (0.2g catalyst; 300 W Xe Lamp; 70min)	[94]
S-scheme	TiO <sub>2</sub> /BaTiO <sub>3</sub>	/	toluene		86.3% (0.1mg catalyst; 300 W High-pressure Mercury Lamp; 1h)	[95]
S-scheme	CeO <sub>2</sub> @CN	/	formaldehyde		100% (0.3g catalyst; Xe Lamp; 100min)	[96]
S-scheme	CeO <sub>2</sub> /Cu <sub>2</sub> O	/	toluene		100% (Xe Lamp; 50min)	[96]

**Table S5.** Application of MOFs materials in photocatalytic degradation of VOCs.

Photocatalyst	Eg(eV)	SBET (m <sup>2</sup> g <sup>-1</sup> )*	Target pollutants	Pollutant Degradation Effect	Ref.
---------------	--------	---	-------------------	------------------------------	------

UiO-66/TiO <sub>2</sub>	/	1432.7	dimethyl sulphide (DMS)	99% (UV Lamp; 80min)	[97]
MXene(Ti <sub>3</sub> C <sub>2</sub> )/NH <sub>2</sub> -UiO-66	2.4	1391	acetone (CH <sub>3</sub> COCH <sub>3</sub> )	95% (0.1g catalyst; Xe Lamp; 60min)	[98]
TiO <sub>2</sub> /NH <sub>2</sub> -UiO-66	2.82	/	styrene	99% (0.1g catalyst; 300W Xe Lamp; 10h)	[99]
AUiO-66(Zr/Ti)	2.78	413	toluene	80%(0.1g catalyst; 350W Xe Lamp;3h)	[100]
Br <sub>0.2</sub> @UiO-66	3.97	/	acetaldehyde	95% (0.1g catalyst; 125 W Mercury Lamp; 1h)	[101]
TiO <sub>2</sub> -UiO-66-NH <sub>2</sub>	2.96	1121	toluene	90%(0.1g catalyst; 125 W Mercury Lamp;)	[102]
micro-mesoporous UiO-66	/	1240	toluene	Capacity (mg g <sup>-1</sup> ): 394	[103]
ZIF-67/PDA	1.84	662.65	toluene	78.9% (30mg catalyst; 500W Xe Lamp; 6h)	[104]
GC-N-TiO <sub>2</sub>	2.76	/	toluene	100% (50mg catalyst; 300W Xe Lamp; 1h)	[105]
Zn-His-GQDs	/	63.3	Toluene Tthyl acetate	Capacity (mg g <sup>-1</sup> ): 350 and 669 (0.2g catalyst)	[106]
Au@ZnO/ZIF-8	/	923.75	formaldehyde	/	[107]
P-NH <sub>2</sub> -MIL-125	2.53	1423	toluene chlorobenzene	91.9% and 100% (10mg catalyst; 300W Xe Lamp; 1h)	[108]
Disk-like N-TiO <sub>2</sub>	2.87	/	toluene	99.1% (0.05g catalyst; 100W LED Lamp; 8h)	[109]
MIL-125(N-Ti9Zn)	1.85	1415–1419	CH <sub>3</sub> CHO	99% (0.1g catalyst; vis-light; 25min)	[73]
MIL-100(Fe)	2.74	/	acetone	90% (25mg catalyst; 300W Xe Lamp; 1h)	[110]
MIL-100(Fe)/α-Fe <sub>2</sub> O <sub>3</sub>	/	1138	o-xylene	100% (95mg catalyst; 250W Xe Lamp; 5h)	[111]
MIL-101/TiO <sub>2</sub> /PDVB	/	461.47	toluene	90.67% (100mg catalyst; 125 W Mercury Lamp; 8h)	[76]
NaFe-MOXs	2.66	554	acetaldehyde	65%(50mg catalyst; 300W Xe Lamp; 140min)	[112]

\* BET specific surface area

## Reference

1. Carp, O.; Huisman, C.L.; Reller, A. Photoinduced reactivity of titanium dioxide. *Progress in Solid State Chemistry* **2004**, *32*, 33-177, doi:10.1016/j.progsolidstchem.2004.08.001.
2. Pelaez, M.; Nolan, N.T.; Pillai, S.C.; Seery, M.K.; Falaras, P.; Kontos, A.G.; Dunlop, P.S.M.; Hamilton, J.W.J.; Byrne, J.A.; O'Shea, K.; et al. A review on the visible light active titanium dioxide photocatalysts for environmental applications. *Applied Catalysis B: Environmental* **2012**, *125*, 331-349, doi:10.1016/j.apcatb.2012.05.036.
3. Montini, T.; Melchionna, M.; Monai, M.; Fornasiero, P. Fundamentals and Catalytic Applications of CeO<sub>2</sub>-Based Materials. *Chemical Reviews* **2016**, *116*, 5987-6041, doi:10.1021/acs.chemrev.5b00603.
4. Pan, X.; Yang, M.-Q.; Fu, X.; Zhang, N.; Xu, Y.-J. Defective TiO<sub>2</sub> with oxygen vacancies: synthesis, properties and photocatalytic applications. *Nanoscale* **2013**, *5*, 3601-3614, doi:10.1039/C3NR00476G.
5. Saunders, S.M.; Jenkin, M.E.; Derwent, R.G.; Pilling, M.J. Protocol for the development of the Master Chemical Mechanism, MCM v3 (Part A): tropospheric degradation of non-aromatic volatile organic compounds. *Atmos. Chem. Phys.* **2003**, *3*, 161-180, doi:10.5194/acp-3-161-2003.
6. Zhao, J.; Yang, X. Photocatalytic oxidation for indoor air purification: a literature review. *Building and Environment* **2003**, *38*, 645-654, doi:10.1016/S0360-1323(02)00212-3.
7. Mo, J.; Zhang, Y.; Xu, Q.; Lamson, J.J.; Zhao, R. Photocatalytic purification of volatile organic compounds in indoor air: A literature review. *Atmospheric Environment* **2009**, *43*, 2229-2246, doi:10.1016/j.atmosenv.2009.01.034.
8. Shayegan, Z.; Lee, C.-S.; Haghghat, F. TiO<sub>2</sub> photocatalyst for removal of volatile organic compounds in gas phase – A review. *Chemical Engineering Journal* **2018**, *334*, 2408-2439, doi:10.1016/j.cej.2017.09.153.
9. Chen, H.; Nanayakkara, C.E.; Grassian, V.H. Titanium Dioxide Photocatalysis in Atmospheric Chemistry. *Chemical Reviews* **2012**, *112*, 5919-5948, doi:10.1021/cr3002092. doi:10.1021/cr3002092.
10. Huang, H.; Xu, Y.; Feng, Q.; Leung, D.Y.C. Low temperature catalytic oxidation of volatile organic compounds: a review. *Catalysis Science & Technology* **2015**, *5*, 2649-2669, doi:10.1039/C4CY01733A.
11. He, Z.-K.; Lu, Y.; Zhao, J.; Zhao, J.; Gao, Z.; Song, Y.-Y. Engineering carrier density at TiO<sub>2</sub> nanotube metasurface with hole reservoir for Enhanced Photo-electrocatalysis. *Applied Surface Science* **2023**, *613*, 155974, doi:10.1016/j.apsusc.2022.155974.
12. Zhang, Y.; Wu, M.; Wang, Y.; Kwok, Y.H.; Pan, W.; Szeto, W.; Huang, H.; Leung, D.Y.C. Fluorinated TiO<sub>2</sub> coupling with α-MnO<sub>2</sub> nanowires supported on different substrates for photocatalytic VOCs abatement under vacuum ultraviolet irradiation. *Applied Catalysis B: Environmental* **2021**, *280*, 119388,

doi:10.1016/j.apcatb.2020.119388.

13. Selishchev, D.; Svintsitskiy, D.; Kovtunova, L.; Gerasimov, E.; Gladky, A.; Kozlov, D. Surface modification of TiO<sub>2</sub> with Pd nanoparticles for enhanced photocatalytic oxidation of benzene micropollutants. *Colloids and Surfaces A: Physicochemical and Engineering Aspects* **2021**, *612*, 125959, doi:10.1016/j.colsurfa.2020.125959.
14. Shayegan, Z.; Haghghat, F.; Lee, C.-S. Surface fluorinated Ce-doped TiO<sub>2</sub> nanostructure photocatalyst: A trap and remove strategy to enhance the VOC removal from indoor air environment. *Chemical Engineering Journal* **2020**, *401*, 125932, doi:10.1016/j.cej.2020.125932.
15. Lyu, J.; Zhou, L.; Shao, J.; Zhou, Z.; Gao, J.; Li, J.; Dong, Y.; Wang, Z. Synthesis of TiO<sub>2</sub>/H<sub>2</sub>Ti<sub>3</sub>O<sub>7</sub> composite with nanoscale spiny hollow hierarchical structure for photocatalytic mineralization of VOCs. *Chemical Engineering Journal* **2020**, *400*, 125927, doi:10.1016/j.cej.2020.125927.
16. Fujimoto, T.M.; Ponczek, M.; Rochetto, U.L.; Landers, R.; Tomaz, E. Photocatalytic oxidation of selected gas-phase VOCs using UV light, TiO<sub>2</sub>, and TiO<sub>2</sub>/Pd. *Environmental Science and Pollution Research* **2017**, *24*, 6390–6396, doi:10.1007/s11356-016-6494-7.
17. Degefu, D.M.; Liao, Z. Photocatalytic degradation of volatile organic compounds using nanocomposite of P-type and N-type transition metal semiconductors. *Journal of Sol-Gel Science and Technology* **2021**, *98*, 605–614, doi:10.1007/s10971-021-05532-y.
18. Mishra, A.; Mehta, A.; Kainth, S.; Basu, S. Effect of different plasmonic metals on photocatalytic degradation of volatile organic compounds (VOCs) by bentonite/M-TiO<sub>2</sub> nanocomposites under UV/visible light. *Applied Clay Science* **2018**, *153*, 144–153, doi:10.1016/j.clay.2017.11.040.
19. Fiorenza, R.; Bellardita, M.; D'Urso, L.; Compagnini, G.; Palmisano, L.; Scirè, S. Au/TiO<sub>2</sub>-CeO<sub>2</sub> Catalysts for Photocatalytic Water Splitting and VOCs Oxidation Reactions. *Catalysts* **2016**, *6*, 121. doi:10.3390/catal6080121.
20. Shayegan, Z.; Haghghat, F.; Lee, C.-S. Carbon-doped TiO<sub>2</sub> film to enhance visible and UV light photocatalytic degradation of indoor environment volatile organic compounds. *Journal of Environmental Chemical Engineering* **2020**, *8*, 104162, doi:10.1016/j.jece.2020.104162.
21. Le Thi Hoang, Y.; Van Thuan, D.; Hanh, N.T.; Vy, N.H.T.; Hang, T.T.M.; Van Ha, H.; Pham, T.-D.; Sharma, A.K.; Nguyen, M.-V.; Dang, N.-M.; et al. Synthesis of N and S Co-doped TiO<sub>2</sub> Nanotubes for Advanced Photocatalytic Degradation of Volatile Organic Compounds (VOCs) in Gas Phase. *Topics in Catalysis* **2020**, *63*, 1077–1085, doi:10.1007/s11244-020-01347-3.
22. Shayegan, Z.; Haghghat, F.; Lee, C.-S. Anatase/brookite biphasic surface fluorinated Fe–TiO<sub>2</sub> photocatalysts to enhance photocatalytic removal of VOCs under visible and UV light. *Journal of Cleaner Production* **2021**, *287*, 125462, doi:10.1016/j.jclepro.2020.125462.
23. Wu, Q.; Ye, J.; Qiao, W.; Li, Y.; Niemantsverdriet, J.W.; Richards, E.; Pan, F.; Su, R. Inhibit the formation of toxic methylphenolic by-products in photo-decomposition of formaldehyde – toluene/xylene mixtures by Pd

- cocatalyst on TiO<sub>2</sub>. *Applied Catalysis B: Environmental* **2021**, *291*, 120118, doi:10.1016/j.apcatb.2021.120118.
24. Shu, Y.; Ji, J.; Xu, Y.; Deng, J.; Huang, H.; He, M.; Leung, D.Y.C.; Wu, M.; Liu, S.; Liu, S.; et al. Promotional role of Mn doping on catalytic oxidation of VOCs over mesoporous TiO<sub>2</sub> under vacuum ultraviolet (VUV) irradiation. *Applied Catalysis B: Environmental* **2018**, *220*, 78-87, doi:10.1016/j.apcatb.2017.08.019.
  25. Rangkooy, H.A.; Ghaedi, H.; Jahani, F. Removal of xylene vapor pollutant from the air using new hybrid substrates of TiO<sub>2</sub>-WO<sub>3</sub> nanoparticles immobilized on the ZSM-5 zeolite under UV radiation at ambient temperature: Experimental towards modeling. *Journal of Environmental Chemical Engineering* **2019**, *7*, 103247, doi:10.1016/j.jece.2019.103247.
  26. Zhao, X.; Wu, M.; Zhang, Y.; Szeto, W.; Wang, Y.; Pan, W.; Li, J.; Leung, D.Y.C. Bifunctional Mn<sup>2+</sup> grafted Ultra-small TiO<sub>2</sub> nanoparticles on carbon cloth with efficient toluene degradation in a continuous flow reactor. *Chemical Engineering Science* **2022**, *250*, 117389, doi:10.1016/j.ces.2021.117389.
  27. Roso, M.; Boaretti, C.; Bonora, R.; Modesti, M.; Lorenzetti, A. Nanostructured Active Media for Volatile Organic Compounds Abatement: the Synergy of Graphene Oxide and Semiconductor Coupling. *Industrial & Engineering Chemistry Research* **2018**, *57*, 16635-16644, doi:10.1021/acs.iecr.8b04134.
  28. Chen, J.; Chen, L.; Wang, X.; Rao, Z.; Sun, J.; Chen, A.; Xie, X. Rare-earth single atoms decorated 2D-TiO<sub>2</sub> nanosheets for the photodegradation of gaseous O-xylene. *Journal of Colloid and Interface Science* **2022**, *605*, 674-684, doi:10.1016/j.jcis.2021.07.129.
  29. Mahmood, A.; Shi, G.; Wang, Z.; Rao, Z.; Xiao, W.; Xie, X.; Sun, J. Carbon quantum dots-TiO<sub>2</sub> nanocomposite as an efficient photocatalyst for the photodegradation of aromatic ring-containing mixed VOCs: An experimental and DFT studies of adsorption and electronic structure of the interface. *Journal of Hazardous Materials* **2021**, *401*, 123402, doi:10.1016/j.jhazmat.2020.123402.
  30. Hu, Y.; Chen, W.; Fu, J.; Ba, M.; Sun, F.; Zhang, P.; Zou, J. Hydrothermal synthesis of BiVO<sub>4</sub>/TiO<sub>2</sub> composites and their application for degradation of gaseous benzene under visible light irradiation. *Applied Surface Science* **2018**, *436*, 319-326, doi:10.1016/j.apsusc.2017.12.054.
  31. Ren, C.; Qiu, W.; Zhang, H.; He, Z.; Chen, Y. Degradation of benzene on TiO<sub>2</sub>/SiO<sub>2</sub>/Bi<sub>2</sub>O<sub>3</sub> photocatalysts under UV and visible light. *Journal of Molecular Catalysis A: Chemical* **2015**, *398*, 215-222, doi:10.1016/j.molcata.2014.12.007.
  32. Sun, S.; Ding, J.; Bao, J.; Gao, C.; Qi, Z.; Yang, X.; He, B.; Li, C. Photocatalytic degradation of gaseous toluene on Fe-TiO<sub>2</sub> under visible light irradiation: A study on the structure, activity and deactivation mechanism. *Applied Surface Science* **2012**, *258*, 5031-5037. doi:10.1016/j.apsusc.2012.01.075.
  33. Kannangara, Y.Y.; Wijesena, R.; Rajapakse, R.M.G.; de Silva, K.M.N. Heterogeneous photocatalytic degradation of toluene in static environment employing thin films of nitrogen-doped nano-titanium dioxide. *International Nano Letters* **2018**, *8*, 31-39, doi:10.1007/s40089-018-0230-x.
  34. Li, J.-J.; Cai, S.-C.; Xu, Z.; Chen, X.; Chen, J.; Jia, H.-P.; Chen, J. Solvothermal

- syntheses of Bi and Zn co-doped TiO<sub>2</sub> with enhanced electron-hole separation and efficient photodegradation of gaseous toluene under visible-light. *Journal of Hazardous Materials* **2017**, *325*, 261–270, doi:10.1016/j.jhazmat.2016.12.004.
35. Cheng, Y.; Gao, X.; Zhang, X.; Su, J.; Wang, G.; Wang, L. Synthesis of a TiO<sub>2</sub>–Cu<sub>2</sub>O composite catalyst with enhanced visible light photocatalytic activity for gas-phase toluene. *New Journal of Chemistry* **2018**, *42*, 9252–9259, doi:10.1039/C8NJ00409A.
  36. Khan, R.; Kim, T.-J. Preparation and application of visible-light-responsive Ni-doped and SnO<sub>2</sub>-coupled TiO<sub>2</sub> nanocomposite photocatalysts. *Journal of Hazardous Materials* **2009**, *163*, 1179–1184, doi:10.1016/j.jhazmat.2008.07.078.
  37. Qu, X.-G.; Liu, W.-X.; Ma, J.; Cao, W. Research on photodegradation of formaldehyde by nanocrystalline N-TiO<sub>2</sub> powders under visible light irradiation. *Research on Chemical Intermediates* **2009**, *35*, 313–320, doi:10.1007/s11164-009-0026-8.
  38. Hu, Y.; Song, X.; Jiang, S.; Wei, C. Enhanced photocatalytic activity of Pt-doped TiO<sub>2</sub> for NO<sub>x</sub> oxidation both under UV and visible light irradiation: A synergistic effect of lattice Pt<sup>4+</sup> and surface PtO. *Chemical Engineering Journal* **2015**, *274*, 102–112, doi:10.1016/j.cej.2015.03.135.
  39. Yao, J.; Zhang, Y.; Wang, Y.; Chen, M.; Huang, Y.; Cao, J.; Ho, W.; Lee, S.C. Enhanced photocatalytic removal of NO over titania/hydroxyapatite (TiO<sub>2</sub>/HAp) composites with improved adsorption and charge mobility ability. *RSC advances* **2017**, *7*, 24683–24689. doi:10.1039/c7ra02157g
  40. Selishchev, D.S.; Filippov, T.N.; Lyulyukin, M.N.; Kozlov, D.V. Uranyl-modified TiO<sub>2</sub> for complete photocatalytic oxidation of volatile organic compounds under UV and visible light. *Chemical Engineering Journal* **2019**, *370*, 1440–1449, doi:10.1016/j.cej.2019.03.280.
  41. Wang, C.; Rao, Z.; Mahmood, A.; Wang, X.; Wang, Y.; Xie, X.; Sun, J. Improved photocatalytic oxidation performance of gaseous acetaldehyde by ternary g-C<sub>3</sub>N<sub>4</sub>/Ag-TiO<sub>2</sub> composites under visible light. *Journal of Colloid and Interface Science* **2021**, *602*, 699–711, doi:10.1016/j.jcis.2021.05.186.
  42. Xue, X.; Chen, X.; Gong, X. Fast electron transfer and enhanced visible light photocatalytic activity of silver and Ag<sub>2</sub>O co-doped titanium dioxide with the doping of electron mediator for removing gaseous toluene. *Materials Science in Semiconductor Processing* **2021**, *132*, 105901, doi:10.1016/j.mssp.2021.105901.
  43. Yang, S.-B.; Chun, H.-H.; Tayade, R.J.; Jo, W.-K. Iron-functionalized titanium dioxide on flexible glass fibers for photocatalysis of benzene, toluene, ethylbenzene, and o-xylene (BTEX) under visible- or ultraviolet-light irradiation. *Journal of the Air & Waste Management Association* **2015**, *65*, 365–373, doi:10.1080/10962247.2014.995838.
  44. Cherni, D.; Moussa, N.; Nsib, M.F.; Olivo, A.; Signoretto, M.; Prati, L.; Villa, A. Photocatalytic degradation of ethylbenzene in gas phase over N or NF doped TiO<sub>2</sub> catalysts. *Journal of Materials Science: Materials in Electronics* **2019**, *30*, 18919–18926, doi:10.1007/s10854-019-02248-2.
  45. Chen, Y.; Cao, X.; Gao, B.; Lin, B. A facile approach to synthesize N-doped and



- oxygen-deficient TiO<sub>2</sub> with high visible-light activity for benzene decomposition. *Materials Letters* **2013**, *94*, 154-157. doi:10.1016/j.matlet.2012.12.010.
46. Xie, R.; Lei, D.; Zhan, Y.; Liu, B.; Tsang, C.H.A.; Zeng, Y.; Li, K.; Leung, D.Y.C.; Huang, H. Efficient photocatalytic oxidation of gaseous toluene over F-doped TiO<sub>2</sub> in a wet scrubbing process. *Chemical Engineering Journal* **2020**, *386*, 121025, doi:10.1016/j.cej.2019.02.112.
47. Zhang, Y.; Wu, M.; Kwok, Y.H.; Wang, Y.; Zhao, W.; Zhao, X.; Huang, H.; Leung, D.Y.C. In-situ synthesis of heterojunction TiO<sub>2</sub>/MnO<sub>2</sub> nanostructure with excellent performance in vacuum ultraviolet photocatalytic oxidation of toluene. *Applied Catalysis B: Environmental* **2019**, *259*, 118034, doi:10.1016/j.apcatb.2019.118034.
48. Dai, X.; Lu, G.; Hu, Y.; Xie, X.; Wang, X.; Sun, J. Reversible redox behavior of Fe<sub>2</sub>O<sub>3</sub>/TiO<sub>2</sub> composites in the gaseous photodegradation process. *Ceramics International* **2019**, *45*, 13187-13192, doi:10.1016/j.ceramint.2019.03.255.
49. Zhou, W.; Shen, B.; Wang, F.; Zhang, X.; Zhao, Z.; Si, M.; Guo, S. Enhanced photocatalytic degradation of xylene by blackening TiO<sub>2</sub> nanoparticles with high dispersion of CuO. *Journal of Hazardous Materials* **2020**, *391*, 121642, doi:10.1016/j.jhazmat.2019.121642.
50. Kong, J.; Lai, X.; Rui, Z.; Ji, H.; Ji, S. Multichannel charge separation promoted ZnO/P<sub>25</sub> heterojunctions for the photocatalytic oxidation of toluene. *Chinese Journal of Catalysis* **2016**, *37*, 869-877, doi:10.1016/S1872-2067(15)61093-2.
51. Koli, V.B.; Kim, J.-S. Photocatalytic oxidation for removal of gases toluene by TiO<sub>2</sub>-CeO<sub>2</sub> nanocomposites under UV light irradiation. *Materials Science in Semiconductor Processing* **2019**, *94*, 70-79, doi:10.1016/j.mssp.2019.01.032.
52. Qu, J.; Chen, D.; Li, N.; Xu, Q.; Li, H.; He, J.; Lu, J. Ternary photocatalyst of atomic-scale Pt coupled with MoS<sub>2</sub> co-loaded on TiO<sub>2</sub> surface for highly efficient degradation of gaseous toluene. *Applied Catalysis B: Environmental* **2019**, *256*, 117877, doi:10.1016/j.apcatb.2019.117877.
53. Xin, Y.; Chen, Q.; Zhang, G. Construction of ternary heterojunction CuS-CdS/TiO<sub>2</sub> nanobelts for photocatalytic degradation of gaseous toluene. *Journal of Alloys and Compounds* **2018**, *751*, 231-240, doi:10.1016/j.jallcom.2018.04.116.
54. Hua, J.; Wang, M.; Jiao, Y.; Li, H.; Yang, Y. Strongly coupled CdX (XS, Se and Te) quantum dots/TiO<sub>2</sub> nanocomposites for photocatalytic degradation of benzene under visible light irradiation. *Optik* **2018**, *171*, 95-106, doi:10.1016/j.ijleo.2018.06.049.
55. Caudillo-Flores, U.; Muñoz-Batista, M.J.; Luque, R.; Fernández-García, M.; Kubacka, A. g-C<sub>3</sub>N<sub>4</sub>/TiO<sub>2</sub> composite catalysts for the photo-oxidation of toluene: Chemical and charge handling effects. *Chemical Engineering Journal* **2019**, *378*, 122228, doi:10.1016/j.cej.2019.122228.
56. Huang, H.; Li, D.; Lin, Q.; Zhang, W.; Shao, Y.; Chen, Y.; Sun, M.; Fu, X. Efficient Degradation of Benzene over LaVO<sub>4</sub>/TiO<sub>2</sub> Nanocrystalline Heterojunction Photocatalyst under Visible Light Irradiation. *Environmental Science & Technology* **2009**, *43*, 4164-4168, doi:10.1021/es900393h.
57. Huang, Q.; Zhang, Q.; Yuan, S.; Zhang, Y.; Zhang, M. One-pot facile synthesis of branched Ag-ZnO heterojunction nanostructure as highly efficient

- photocatalytic catalyst. *Applied Surface Science* **2015**, *353*, 949–957, doi:10.1016/j.apsusc.2015.06.197.
58. Chen, Y.-C.; Katsumata, K.-i.; Chiu, Y.-H.; Okada, K.; Matsushita, N.; Hsu, Y.-J. ZnO–graphene composites as practical photocatalysts for gaseous acetaldehyde degradation and electrolytic water oxidation. *Applied Catalysis A: General* **2015**, *490*, 1–9, doi:10.1016/j.apcata.2014.10.055.
59. Jafari, A.J.; Kalantary, R.R.; Esrafil, A.; Arfaeinia, H. Synthesis of silica-functionalized graphene oxide/ZnO coated on fiberglass and its application in photocatalytic removal of gaseous benzene. *Process Safety and Environmental Protection* **2018**, *116*, 377–387, doi:10.1016/j.psep.2018.03.015.
60. Liu, J.; Wang, P.; Qu, W.; Li, H.; Shi, L.; Zhang, D. Nanodiamond-decorated ZnO catalysts with enhanced photocorrosion-resistance for photocatalytic degradation of gaseous toluene. *Applied Catalysis B: Environmental* **2019**, *257*, 117880, doi:10.1016/j.apcatb.2019.117880.
61. Ji, W.; Shen, T.; Kong, J.; Rui, Z.; Tong, Y. Synergistic Performance between Visible-Light Photocatalysis and Thermocatalysis for VOCs Oxidation over Robust Ag/F-Codoped SrTiO<sub>3</sub>. *Industrial & Engineering Chemistry Research* **2018**, *57*, 12766–12773, doi:10.1021/acs.iecr.8b02873.
62. Zou, X.; Yuan, C.; Cui, Y.; Dong, Y.; Chen, D.; Ge, H.; Ke, J. Construction of zinc-indium-sulfide/indium oxide step-scheme junction catalyst for enhanced photocatalytic activities of pollutant degradation and hydrogen generation. *Separation and Purification Technology* **2021**, *266*, 118545, doi:10.1016/j.seppur.2021.118545.
63. Pham, T.-H.; Jung, S.H.; Kim, T. Enhanced photodegradation of toxic volatile organic pollutants using Ni-doped graphitic carbon nitride under natural solar light. *Solar Energy* **2021**, *224*, 18–26, doi:10.1016/j.solener.2021.05.087.
64. Li, X.; Fang, G.; Qian, X.; Tian, Q. Z-scheme heterojunction of low conduction band potential MnO<sub>2</sub> and biochar-based g-C<sub>3</sub>N<sub>4</sub> for efficient formaldehyde degradation. *Chemical Engineering Journal* **2022**, *428*, 131052, doi:10.1016/j.cej.2021.131052.
65. Meng, J.; Wang, X.; Yang, X.; Hu, A.; Guo, Y.; Yang, Y. Enhanced gas-phase photocatalytic removal of aromatics over direct Z-scheme-dictated H<sub>3</sub>PW<sub>12</sub>O<sub>40</sub>/g-C<sub>3</sub>N<sub>4</sub> film-coated optical fibers. *Applied Catalysis B: Environmental* **2019**, *251*, 168–180, doi:10.1016/j.apcatb.2019.03.063.
66. Wu, P.; Dai, S.; Chen, G.; Zhao, S.; Xu, Z.; Fu, M.; Chen, P.; Chen, Q.; Jin, X.; Qiu, Y.; et al. Interfacial effects in hierarchically porous α-MnO<sub>2</sub>/Mn<sub>3</sub>O<sub>4</sub> heterostructures promote photocatalytic oxidation activity. *Applied Catalysis B: Environmental* **2020**, *268*, 118418, doi:10.1016/j.apcatb.2019.118418.
67. Wu, M.; Zhang, Y.; Szeto, W.; Pan, W.; Huang, H.; Leung, D.Y.C. Vacuum ultraviolet (VUV)-based photocatalytic oxidation for toluene degradation over pure CeO<sub>2</sub>. *Chemical Engineering Science* **2019**, *200*, 203–213, doi:10.1016/j.ces.2019.01.056.
68. Park, B.-G. Photoluminescence of Eu<sup>3+</sup>-doped CaTiO<sub>3</sub> perovskites and their photocatalytic properties with a metal ion loading. *Chemical Physics Letters* **2019**,

- 722, 44-49, doi:10.1016/j.cplett.2019.03.007.
69. Yang, X.; Liu, S.; Li, J.; Chen, J.; Rui, Z. Promotion effect of strong metal-support interaction to thermocatalytic, photocatalytic, and photothermocatalytic oxidation of toluene on Pt/SrTiO<sub>3</sub>. *Chemosphere* **2020**, *249*, 126096, doi:10.1016/j.chemosphere.2020.126096.
  70. Miodyńska, M.; Bajorowicz, B.; Mazierski, P.; Lisowski, W.; Klimczuk, T.; Winiarski, M.J.; Zaleska-Medynska, A.; Nadolna, J. Preparation and photocatalytic properties of BaZrO<sub>3</sub> and SrZrO<sub>3</sub> modified with Cu<sub>2</sub>O/Bi<sub>2</sub>O<sub>3</sub> quantum dots. *Solid State Sciences* **2017**, *74*, 13-23, doi:10.1016/j.solidstatesciences.2017.10.003.
  71. Krukowska, A.; Trykowski, G.; Lisowski, W.; Klimczuk, T.; Winiarski, M.J.; Zaleska-Medynska, A. Monometallic nanoparticles decorated and rare earth ions doped KTaO<sub>3</sub>/K<sub>2</sub>Ta<sub>2</sub>O<sub>6</sub> photocatalysts with enhanced pollutant decomposition and improved H<sub>2</sub> generation. *Journal of Catalysis* **2018**, *364*, 371-381, doi:10.1016/j.jcat.2018.05.013.
  72. Mehrzadeh, H.; Niaei, A.; Tseng, H.-H.; Salari, D.; Khataee, A. Synthesis of ZnFe<sub>2</sub>O<sub>4</sub> nanoparticles for photocatalytic removal of toluene from gas phase in the annular reactor. *Journal of Photochemistry and Photobiology A: Chemistry* **2017**, *332*, 188-195, doi:10.1016/j.jphotochem.2016.08.028.
  73. Gao, Z.; Wang, J.X.; Muhammad, Y.; Zhang, Y.B.; Shah, S.J.; Hu, Y.; Chu, Z.; Zhao, Z.X.; Zhao, Z.X. Enhanced moisture-resistance and excellent photocatalytic performance of synchronous N/Zn-decorated MIL-125(Ti) for vaporous acetaldehyde degradation. *Chemical Engineering Journal* **2020**, *388*, doi:10.1016/j.cej.2020.124389.
  74. Sun, R.; Shi, Q.; Zhang, M.; Xie, L.; Chen, J.; Yang, X.; Chen, M.; Zhao, W. Enhanced photocatalytic oxidation of toluene with a coral-like direct Z-scheme BiVO<sub>4</sub>/g-C<sub>3</sub>N<sub>4</sub> photocatalyst. *Journal of Alloys and Compounds* **2017**, *714*, 619-626, doi:10.1016/j.jallcom.2017.04.108.
  75. Duan, J.; Song, X.; Zhao, H.; Zhang, Z.; Wang, W. Self-assembled flower-like (BiO)<sub>2</sub>CO<sub>3</sub>-CdS-CuS stable heterojunction degrades toluene under visible light response. *Optical Materials* **2020**, *101*, 109761, doi:10.1016/j.optmat.2020.109761.
  76. Yang, Z.X.; Zhang, J.H.; Wang, J.; Hu, Y. Sandwich-like photocatalyst MIL-101@TiO<sub>2</sub>@PDVB with water resistance for efficient oxidation of toluene. *Chemosphere* **2022**, *296*, doi:10.1016/j.chemosphere.2022.133921.
  77. Zou, X.J.; Dong, Y.Y.; Ke, J.; Ge, H.; Chen, D.; Sun, H.J.; Cui, Y.B. Cobalt monoxide/tungsten trioxide p-n heterojunction boosting charge separation for efficient visible-light-driven gaseous toluene degradation. *Chemical Engineering Journal* **2020**, *400*, doi:10.1016/j.cej.2020.125919.
  78. Tai, X.H.; Lai, C.W.; Yang, T.C.K.; Johan, M.R.; Lee, K.M.; Chen, C.Y.; Juan, J.C. Highly effective removal of volatile organic pollutants with p-n heterojunction photoreduced graphene oxide-TiO<sub>2</sub> photocatalyst. *Journal of Environmental Chemical Engineering* **2022**, *10*, doi:10.1016/j.jece.2022.107304.
  79. Wang, J.M.; Xu, X.C.; Cao, F.; Wang, Y.A.; Li, S.; Qin, G.W. In situ fabrication of α-Fe<sub>2</sub>O<sub>3</sub>/CaFe<sub>2</sub>O<sub>4</sub> p-n heterojunction with enhanced VOCs photodegradation

- activity. *Advanced Powder Technology* **2019**, *30*, 590-595, doi:10.1016/j.appt.2018.11.027.
80. Xue, X.L.; Gong, X.W.; Chen, X.Y.; Chen, B.Y. A facile synthesis of Ag/Ag<sub>2</sub>O@TiO<sub>2</sub> for toluene degradation under UV-visible light: Effect of Ag formation by partial reduction of Ag<sub>2</sub>O on photocatalyst stability. *Journal of Physics and Chemistry of Solids* **2021**, *150*, doi:10.1016/j.jpcs.2020.109799.
81. Zou, X.J.; Yuan, C.Y.; Dong, Y.Y.; Ge, H.; Ke, J.; Cui, Y.B. Lanthanum orthovanadate/bismuth oxybromide heterojunction for enhanced photocatalytic air purification and mechanism exploration. *Chemical Engineering Journal* **2020**, *379*, doi:10.1016/j.cej.2019.122380.
82. Luo, S.; Ke, J.; Yuan, M.Q.; Zhang, Q.; Xie, P.; Deng, L.D.; Wang, S.B. CuInS<sub>2</sub> quantum dots embedded in Bi<sub>2</sub>WO<sub>6</sub> nanoflowers for enhanced visible light photocatalytic removal of contaminants. *Applied Catalysis B-Environmental* **2018**, *221*, 215-222, doi:10.1016/j.apcatb.2017.09.028.
83. Shi, Z.K.; Lan, L.; Li, Y.Z.; Yang, Y.; Zhang, Q.; Wu, J.C.; Zhang, G.Q.; Zhao, X.J. Co<sub>3</sub>O<sub>4</sub>/TiO<sub>2</sub> Nanocomposite Formation Leads to Improvement in Ultraviolet-Visible-Infrared-Driven Thermocatalytic Activity Due to Photoactivation and Photocatalysis-Thermocatalysis Synergetic Effect. *Acs Sustainable Chemistry & Engineering* **2018**, *6*, 16503-16514, doi:10.1021/acssuschemeng.8b03602.
84. Cheng, Y.Q.; Gao, X.; Zhang, X.X.; Su, J.X.; Wang, G.Q.; Wang, L.Y. Synthesis of a TiO<sub>2</sub>-Cu<sub>2</sub>O composite catalyst with enhanced visible light photocatalytic activity for gas-phase toluene. *New Journal of Chemistry* **2018**, *42*, 9252-9259, doi:10.1039/c8nj00409a.
85. Cheng, R.; Wen, J.Y.; Xia, J.C.; Shen, L.J.; Kang, M.; Shi, L.; Zheng, X. Photo-catalytic oxidation of gaseous toluene by Z-scheme Ag<sub>3</sub>PO<sub>4</sub>-g-C<sub>3</sub>N<sub>4</sub> composites under visible light: Removal performance and mechanisms. *Catalysis Today* **2022**, *388-389*, 26-35, doi:10.1016/j.cattod.2021.05.006.
86. Borjigin, B.; Ding, L.; Li, H.Q.; Wang, X.J. A solar light-induced photo-thermal catalytic decontamination of gaseous benzene by using Ag/Ag<sub>3</sub>PO<sub>4</sub>/CeO<sub>2</sub> heterojunction. *Chemical Engineering Journal* **2020**, *402*, doi:10.1016/j.cej.2020.126070.
87. Zhou, H.R.; Wen, Z.P.; Liu, J.; Ke, J.; Duan, X.G.; Wang, S.B. Z-scheme plasmonic Ag decorated WO<sub>3</sub>/Bi<sub>2</sub>WO<sub>6</sub> hybrids for enhanced photocatalytic abatement of chlorinated-VOCs under solar light irradiation. *Applied Catalysis B-Environmental* **2019**, *242*, 76-84, doi:10.1016/j.apcatb.2018.09.090.
88. Li, X.; Fang, G.G.; Qian, X.R.; Tian, Q.W. Z-scheme heterojunction of low conduction band potential MnO<sub>2</sub> and biochar-based g-C<sub>3</sub>N<sub>4</sub> for efficient formaldehyde degradation. *Chemical Engineering Journal* **2022**, *428*, doi:10.1016/j.cej.2021.131052.
89. Yang, J.; Yang, L.; Fang, M.; Li, L.; Fu, F.; Xu, H.; Li, M.G.; Fan, X.M. A compact Z-scheme heterojunction of BiOCl/Bi<sub>2</sub>WO<sub>6</sub> for efficiently photocatalytic degradation of gaseous toluene. *Journal of Colloid and Interface Science* **2023**, *631*, 44-54, doi:10.1016/j.jcis.2022.11.023.

90. Jia, Y.; Zhang, X.; Wang, R.Y.; Yuan, J.; Zheng, R.Z.; Zhang, J.Q.; Qian, F.P.; Chen, Y.F.; Zhang, M.; Guo, L.A. Energy band engineering of  $\text{WO}_3/\text{Bi}_2\text{WO}_6$  direct Z-scheme for enhanced photocatalytic toluene degradation. *Applied Surface Science* **2023**, *618*, doi:10.1016/j.apsusc.2023.156636.
91. Xue, J.Q.; Shi, L.; Wang, P.; Cheng, W.; Long, M.Y.; Sheng, M.J.; Bi, Q. Efficient degradation of VOCs using semi-coke activated carbon loaded 2D Z-scheme  $\text{g-C}_3\text{N}_4\text{-Bi}_2\text{WO}_6$  photocatalysts composites under visible light irradiation. *Separation and Purification Technology* **2023**, *305*, doi:10.1016/j.seppur.2022.122535.
92. Zhang, N.; He, W.J.; Cheng, Z.Y.; Lu, J.L.; Zhou, Y.; Ding, D.N.; Rong, S.P. Construction of  $\alpha\text{-MnO}_2/\text{g-C}_3\text{N}_4$  Z-scheme heterojunction for photothermal synergistic catalytic decomposition of formaldehyde. *Chemical Engineering Journal* **2023**, *466*, doi:10.1016/j.cej.2023.143160.
93. Li, Y.W.; Li, S.Z.; Zhao, M.B.; Ma, W.L. Decahedral  $\text{BiVO}_4/\text{tubular g-C}_3\text{N}_4$  S-scheme heterojunction photocatalyst for formaldehyde removal: Charge transfer pathway and deactivation mechanism. *Separation and Purification Technology* **2023**, *327*, doi:10.1016/j.seppur.2023.124966.
94. Xu, X.Y.; Su, Y.H.; Dong, Y.P.; Luo, X.; Wang, S.H.; Zhou, W.Y.; Li, R.; Homewood, K.P.; Xia, X.H.; Gao, Y.; et al. Designing and fabricating a  $\text{CdS QDs/Bi}_2\text{MoO}_6$  monolayer S-scheme heterojunction for highly efficient photocatalytic  $\text{C}_2\text{H}_4$  degradation under visible light. *Journal of Hazardous Materials* **2022**, *424*, doi:10.1016/j.jhazmat.2021.127685.
95. Zhou, X.; Wang, X.M.; Tan, T.Q.; Ma, H.; Tang, H.Y.; Luo, X.A.; Dong, F.; Yang, Y. Unique S-scheme  $\text{TiO}_2/\text{BaTiO}_3$  heterojunctions promote stable photocatalytic mineralization of toluene in air. *Chemical Engineering Journal* **2023**, *470*, doi:10.1016/j.cej.2023.143933.
96. Ying, T.T.; Liu, W.; Yang, L.X.; Zhang, S.Q.; Wu, Z.Y.; Li, J.Y.; Song, R.J.; Dai, W.L.; Zou, J.P.; Luo, S.L. S-scheme construction boosts highly active self-supporting  $\text{CeO}_2/\text{Cu}_2\text{O}$  photocatalyst for efficient degradation of indoor VOCs. *Separation and Purification Technology* **2024**, *330*, doi:10.1016/j.seppur.2023.125272.
97. Man, Z.; Meng, Y.; Lin, X.C.; Dai, X.R.; Wang, L.P.; Liu, D.Z. Assembling  $\text{UiO-66@TiO}_2$  nanocomposites for efficient photocatalytic degradation of dimethyl sulfide. *Chemical Engineering Journal* **2022**, *431*, doi:10.1016/j.cej.2021.133952.
98. Yu, X.; Hu, Y.; Luan, X.Q.; Shah, S.J.; Liu, L.M.; Li, C.H.; Ren, Y.F.; Zhou, L.Q.; Li, J.; Deng, J.G.; et al. Microwave-assisted construction of MXene/MOF aerogel via N-metal bonds for efficient photodegradation of vapor acetone under high humidity. *Chemical Engineering Journal* **2023**, *476*, doi:10.1016/j.cej.2023.146878.
99. Yao, P.Z.; Liu, H.L.; Wang, D.T.; Chen, J.Y.; Li, G.Y.; An, T.C. Enhanced visible-light photocatalytic activity to volatile organic compounds degradation and deactivation resistance mechanism of titania confined inside a metal-organic framework. *Journal of Colloid and Interface Science* **2018**, *522*, 174-182, doi:10.1016/j.jcis.2018.03.075.

100. Lin, L.Y.; Liu, C.H.; Dang, V.D.; Fu, H.T. Atomically dispersed Ti-O clusters anchored on NH<sub>2</sub>-UiO-66(Zr) as efficient and deactivation-resistant photocatalyst for abatement of gaseous toluene under visible light. *Journal of Colloid and Interface Science* **2023**, *635*, 323-335, doi:10.1016/j.jcis.2022.12.147.
101. Wang, J.; Yang, C.Q.; Fu, M.L.; Ye, D.Q.; Fan, L.; Hu, Y. Derivatives of Br-doped metal-organic framework for improved acetaldehyde adsorption-photocatalytic oxidation. *Science of the Total Environment* **2024**, *932*, doi:10.1016/j.scitotenv.2024.172941.
102. Zhang, J.H.; Hu, Y.; Qin, J.X.; Yang, Z.X.; Fu, M.L. TiO<sub>2</sub>-UiO-66-NH<sub>2</sub> nanocomposites as efficient photocatalysts for the oxidation of VOCs. *Chemical Engineering Journal* **2020**, *385*, doi:10.1016/j.cej.2019.123814.
103. Zhang, X.D.; Yang, Y.; Lv, X.T.; Wang, Y.X.; Liu, N.; Chen, D.; Cui, L.F. Adsorption/desorption kinetics and breakthrough of gaseous toluene for modified microporous-mesoporous UiO-66 metal organic framework. *Journal of Hazardous Materials* **2019**, *366*, 140-150, doi:10.1016/j.jhazmat.2018.11.099.
104. Li, X.Y.; Li, J.A.; Shi, Y.; Zhang, M.M.; Fan, S.Y.; Yin, Z.F.; Qin, M.C.; Lian, T.T.; Li, X.Y. Rational design of cobalt and nitrogen co-doped carbon hollow frameworks for efficient photocatalytic degradation of gaseous toluene. *Journal of Colloid and Interface Science* **2018**, *528*, 45-52, doi:10.1016/j.jcis.2018.05.067.
105. Qin, J.X.; Wang, J.; Yang, J.J.; Hu, Y.; Fu, M.L.; Ye, D.Q. Metal organic framework derivative-TiO<sub>2</sub> composite as efficient and durable photocatalyst for the degradation of toluene. *Applied Catalysis B-Environmental* **2020**, *267*, doi:10.1016/j.apcatb.2020.118667.
106. Cheng, Y.L.; Zhang, Y.; Li, J.X.; Fang, C.Q.; Chen, J.; Zhao, J.R.; Zhao, T.; Zhu, J. Self-assembly of MOFs-like materials by Zn<sup>2+</sup> and histidine functionalized graphene quantum dots for the efficient removal of VOCs simulants. *Diamond and Related Materials* **2023**, *140*, doi:10.1016/j.diamond.2023.110441.
107. Wang, D.W.; Li, Z.W.; Zhou, J.; Fang, H.; He, X.; Jena, P.R.; Zeng, J.B.; Wang, W.N. Simultaneous Detection and Removal of Formaldehyde at Room Temperature: Janus Au@ZnO@ZIF-8 Nanoparticles. *Nano-Micro Letters* **2018**, *10*, doi:10.1007/s40820-017-0158-0.
108. Zhang, X.D.; Yue, K.; Rao, R.Z.; Chen, J.F.; Liu, Q.; Yang, Y.; Bi, F.K.; Wang, Y.X.; Xu, J.C.; Liu, N. Synthesis of acidic MIL-125 from plastic waste: Significant contribution of N orbital for efficient photocatalytic degradation of chlorobenzene and toluene. *Applied Catalysis B-Environmental* **2022**, *310*, doi:10.1016/j.apcatb.2022.121300.
109. Zhao, C.; Wang, Z.H.; Chen, X.; Chu, H.Y.; Fu, H.F.; Wang, C.C. Robust photocatalytic benzene degradation using mesoporous disk-like N-TiO<sub>2</sub> derived from MIL-125(Ti). *Chinese Journal of Catalysis* **2020**, *41*, 1186-1197, doi:10.1016/s1872-2067(19)63516-3.
110. Qin, J.X.; Pei, Y.; Zheng, Y.; Ye, D.Q.; Hu, Y. Fe-MOF derivative photocatalyst with advanced oxygen reduction capacity for indoor pollutants removal. *Applied Catalysis B-Environmental* **2023**, *325*, doi:10.1016/j.apcatb.2022.122346.
111. Chen, L.; Wang, X.; Rao, Z.P.; Tang, Z.X.; Wang, Y.; Shi, G.S.; Lu, G.H.; Xie, X.F.;

Chen, D.L.; Sun, J. In-situ synthesis of Z-Scheme MIL-100(Fe)/  $\alpha$ -Fe<sub>2</sub>O<sub>3</sub> heterojunction for enhanced adsorption and Visible-light photocatalytic oxidation of O-xylene. *Chemical Engineering Journal* **2021**, *416*, doi:10.1016/j.cej.2021.129112.

112. Chen, L.; Wang, X.; Shi, G.S.; Lu, G.H.; Wang, Y.; Xie, X.F.; Chen, D.L.; Sun, J. The regulation of Lewis acid/basic sites in NaFe bimetal MOXs for the controllable photocatalytic degradation of electron-rich/deficient VOCs. *Applied Catalysis B-Environmental* **2023**, *334*, doi:10.1016/j.apcatb.2023.122850.